Eur Biophys J (2004) 33: 462–467
DOI 10.1007/s00249-003-0386-8

BIOPHYSICS LETTER

Iwan A. T. Schaap · Pedro J. de Pablo
Christoph F. Schmidt

Resolving the molecular structure of microtubules under physiological conditions with scanning force microscopy

Received: 14 October 2003 / Revised: 12 December 2003 / Accepted: 15 December 2003 / Published online: 5 February 2004

Abstract We have imaged microtubules, essential structural elements of the cytoskeleton in eukaryotic cells, in physiological conditions by scanning force microscopy. We have achieved molecular resolution without the use of cross-linking and chemical fixation methods. With tip forces below 0.3 nN, protofilaments with ~6 nm separation could be clearly distinguished. Lattice defects in the microtubule wall were directly visible, including point defects and protofilament separations. Higher tip forces destroyed the top half of the microtubules, revealing the inner surface of the substrate-attached protofilaments. Monomers could be resolved on these inner surfaces.

Keywords Atomic force microscopy · Microtubule · Scanning force microscopy

Abbreviations APTS: (3-aminopropyl)triethoxysilane · DETA: N^1-[3-(trimethoxysilyl)propyl]diethylenetriamine · EM: electron microscopy · MT: microtubule · SFM: scanning force microscopy

Introduction

The cytoskeleton of eukaryotic cells is a highly dynamic system, constantly reconstructing itself to perform complicated functions, such as cell growth, locomotion or division. Microtubules (MTs), a central component of this cytoskeleton (Alberts et al. 2002), interact with a multitude of microtubule-associated proteins (Cassimeris and Spittle 2001) and also serve as tracks for molecular motors of the kinesin and dynein families (Hirokawa 1998). MTs are two-dimensional tubular protein polymers and in vivo are commonly composed of 13 parallel protofilaments (Tilney et al. 1973), which are connected laterally into hollow tubes. Protofilaments consist of head-to-tail joined dimers of α- and β-tubulin (55 kD each). The outer diameter of an MT is about 25 nm, while the length can vary from tens of nanometers to tens or even hundreds of micrometers, frequently spanning the whole cell (Alberts et al. 2002).

The atomic structure of tubulin has been solved by electron crystallography (Nogales et al. 1998), followed by a high-resolution 3D electron microscopy (EM) reconstruction of the MT structure (Nogales et al. 1999). The number of protofilaments of in vitro polymerized MTs has been found to vary between 11 and 17, depending on the buffer conditions (Pierson et al. 1978). Transitions have been found within individual MTs, corresponding to line defects in the MT lattice (Chrétien et al. 1992). It has been speculated that there might also be other types of lattice defects, such as point defects, and it has been postulated that the motor-like protein katanin, which catalyzes the breakdown of MTs, specifically targets such defects (Davis et al. 2002).

To precisely understand the many dynamic processes that MTs are involved in, it will be crucial to be able to image with molecular resolution in physiological conditions. EM, which provides molecular resolution, requires fixed and stained or frozen samples, precluding the observation of dynamic processes. Light microscopy, on the other hand, has insufficient resolution to distinguish structures on the scale of the tubulin subunits (4 nm). To study dynamic rearrangements, interactions with motor proteins and regulatory proteins, as well as the dynamic properties of defects in the MT lattice, it is necessary to merge nanometer resolution with the capability to work in a close-to-native environment at room temperature. Scanning force microscopy (SFM) (Binnig et al. 1986) operated in buffer can meet these requirements. SFM

I. A. T. Schaap (✉) · P. J. de Pablo · C. F. Schmidt
Section Physics of Complex Systems,
Department of Physics and Astronomy,
Faculty of Sciences, Vrije Universiteit Amsterdam,
De Boelelaan 1081, 1081 HV Amsterdam, The Netherlands
E-mail: ischaap@nat.vu.nl
Tel.: +31-20-447904
Fax: +31-20-4447991

Present address: P. J. de Pablo
Departamento de Física de la Materia Condensada C-III,
Universidad Autónoma de Madrid, 28049 Madrid, Spain

makes use of a tip with a radius of order 10 nm to mechanically scan the sample, and thereby produces a topographical map. The sample needs to be attached to a (smooth) surface to be imaged. MTs, being hollow shell structures, are very prone to damage. Initial attempts of imaging with SFM in tapping mode were limited in resolution and struggled with the damage problem (Fritz et al. 1995), or had to employ strong cross-linking by glutaraldehyde to reinforce the MTs (Vinckier et al. 1996). The latter method is likely to affect dynamic properties as well as interactions with other proteins.

Here we show that by carefully choosing the method of surface attachment, as well as the method of scanning and controlling the maximal tip force, it is possible to image MTs in buffer with single-protein resolution, without destroying or noticeably deforming them.

Materials and methods

Sample preparation

Tubulin was purified from porcine brain using standard methods (Williams and Lee 1982), and polymerized at 3 mg/ml concentration by adding 10% glycerol and 1 mM GTP followed by incubation at 36 °C for 30 min. MTs were 200-fold diluted into PEM80 buffer (80 mM Pipes, pH 6.9, 1 mM EGTA, 2 mM $MgCl_2$) plus 10 μM paclitaxel (Taxol, Sigma) to prevent depolymerization. To attach the negatively charged MTs, clean glass cover slips were derivatized with a positively charged silane (de Pablo et al. 2003b) by immersing in a 0.1% solution of (3-aminopropyl)triethoxysilane (APTS, Aldrich). They were then rinsed with water and cured at 65 °C. For some samples we used a 1% solution of N^1-[3-(trimethoxysilyl)propyl]diethylenetriamine (DETA, Aldrich) (Turner et al. 1995). The solution was hydrolyzed for 5 min before immersing the cover slips for another 5 min; they were then rinsed with water and cured at 110 °C.

Imaging

A volume of 40 μl of the MT sample was sufficient to create a meniscus between the glass surface and the cantilever holder of the SFM (Nanotec, Spain), submerging the sample and cantilever with tip in buffer. Soft cantilevers (OMCL-RC800PSA, Olympus, Japan) with a spring constant of 0.05 N/m and a tip radius of about 20 nm were used.

Results

Imaging microtubules in liquid

The SFM operating method used here is the "jumping mode", described elsewhere in detail (de Pablo et al. 1998). In this mode the SFM performs a force–distance curve at every point of a raster scan with a maximum vertical force that is set as a parameter (Fig. 1). For each point the vertical sample position at this set force is recorded. The tip is then elevated about 30 nm from the surface before performing the lateral motion to the next point, thereby minimizing lateral drag forces on the sample. Typically we started an experiment by scanning a 3×3 μm^2 area with 256×256 scan points at a set force of about 100 pN. We adjusted the MT concentration by inspection of similarly prepared surfaces in a light microscope, using differential interference contrast microscopy, such that on average about one MT was visible in a 3×3 μm^2 window. We experimented with the surface derivatization method and with sample handling (avoiding excessive shearing) until only a fraction of $< \sim 10\%$ of destroyed MTs was seen in the initial scans. MTs were typically many micrometers long. After selecting one MT, we zoomed in to image with higher resolution in a scan area of 500×500 nm^2. In these repeated scans at low force, an occasional MT was found to disintegrate ($< \sim 10\%$ of the cases).

The MT in Fig. 2A shows a maximum height of 23 nm, close to the 25 nm diameter observed with EM. This suggests that the tip did not indent the MT noticeably. The tip radius of about 20 nm is of the same order of magnitude as the MT diameter. This leads to exaggerated horizontal dimensions in the image, with the sides of the tip contributing to image formation, but this does not affect the measured height of the MT (Villarrubia 1997). The dilation effect is shown schematically in Fig. 2B, resulting here in a measured apparent MT width of 70 nm. Owing to the curvature of the MT surface, the (apparent) lateral spacing between

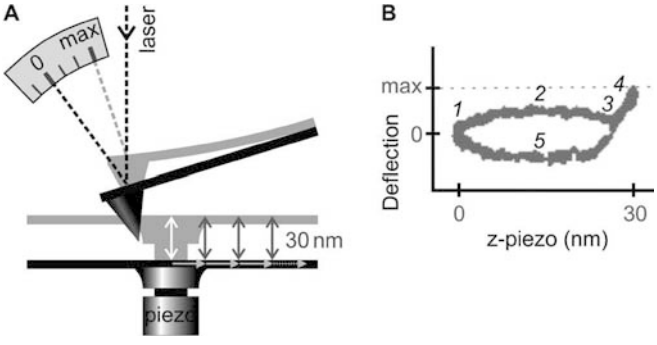

Fig. 1A, B Sketch of the "jumping mode" scanning procedure (not to scale). **A** The cantilever is drawn in two states. *Black*: elevated from the surface, in the position where lateral sample motion occurs. *Gray*: the sample has been moved upwards by the piezo until the tip–sample contact bent the cantilever to the point corresponding to the chosen set force. Cantilever deflection is measured, as common in SFM, by a laser beam, which is reflected onto a split photodiode detector. Because scanning is performed in liquid, there is no capillary tip–surface adhesion force. The *arrows* illustrate the vertical and horizontal motion of the sample while progressing along one scan line. **B** A jump curve as displayed on the oscilloscope (averaged over tens of scan points). *1*. The tip starts at a height of ~30 nm above the sample. *2*. The piezo moves the sample upwards, and the viscous drag on the cantilever causes a small deflection. *3*. The tip contacts the sample. *4*. This is the contact phase. The deflection is linear with the piezo displacement; the maximum allowed deflection is set as a parameter. Once this deflection is reached, the *z*-piezo position is recorded, and the piezo will retract the sample from the tip. *5*. The viscous drag causes an inverted deflection on the way back. At a height of 30 nm the *z*-piezo movement will stop. At this point the piezo will direct the sample by a lateral displacement to the next scan point, were a new force–distance curve is performed. At each scan point, only the piezo *z*-displacement required to reach the set force is recorded

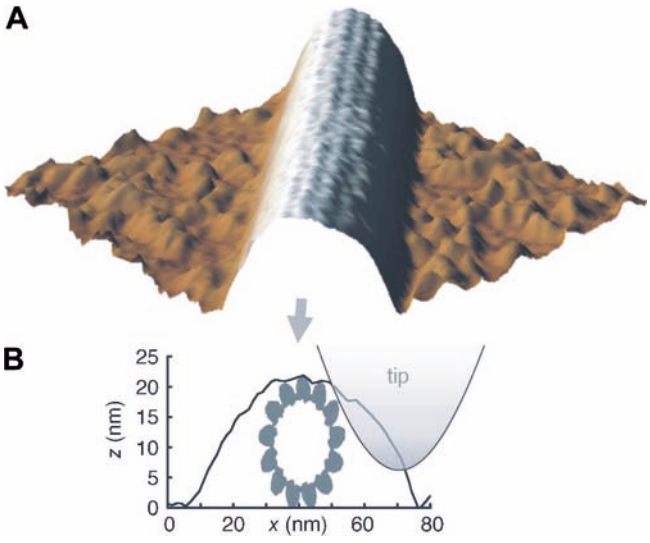

Fig. 2A, B Over 100 scans performed on dozens of different MTs showing protofilaments were recorded during multiple sessions. Each experiment was performed using fresh samples and new tips. **A** 3D-rendered topography map of a 220-nm-long MT segment on an APTS surface, scanned with 100×100 points, applying a maximal force of 90 pN in each point. The protofilaments running parallel to the MT axis are clearly visible. **B** Dilation effect of the tip. The graph shows the profile from **A**, and a tip with 20 nm tip radius. Like in **A**, the *z* and *x* scales are different; therefore the inserted MT cross-section appears deformed

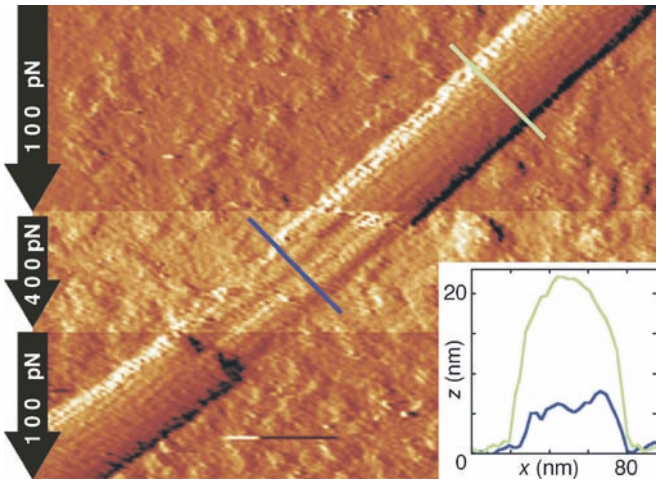

Fig. 3 This image has 256 scan points per 500 nm and was processed with a derivative filter enhancing the edges. The MT attached to an APTS surface is opened intentionally by increasing the scanning force from 100 to 400 pN in the center of the image. The scanning direction was downward with horizontal scan lines. On the horizontal line, where the high force was introduced, a sharp horizontal cut is visible. The region where 400 pN was used is rendered in a brighter color for clarity. The inserted profiles show clearly the difference in height, 23 nm for the intact part and between 5 and 8 nm for the destroyed part, where only some remaining protofilaments can be seen. When the scanning force was reduced again to a low value, the extent to which the high force had disintegrated the MT can be seen. A few scan lines were required before an intact MT was found back

protofilaments grows from ~6 nm to ~9 nm, while the depth of the grooves between protofilaments is underreported as the tip can hardly enter them. Because the sharpest part of the tip is in contact only with the top of the MT, resolution is highest there and decreases towards the sides. In most MTs we could resolve the upper five protofilaments.

Effects of maximal tip force

In order to probe the deformability and the destruction threshold of MTs, we performed scans with increasing maximal tip forces. Scanning with forces exceeding 300 pN as well as running multiple scans with forces close to this value damaged the MTs irreversibly. Figure 3 shows that scanning with high forces tended to destroy the top halves of the MTs, whereupon the rougher inner surface of the bottom half, which was directly attached to the substrate, was imaged. Since no substantial lateral forces are exerted on the MTs while scanning in jumping mode, we suspect that the normal forces were in this case high enough to disrupt lateral and axial bonds between tubulin dimers, such that the whole top halves of the microtubules treated with such forces were disintegrated. With our cantilevers, a minimum force of 50 pN was required to overcome (thermal) noise and assure contact between the tip and the MT, a limit determined by tip and cantilever size, and detection bandwidth (Gittes and Schmidt 1998). The MTs were deformed elastically for tip forces between 50 and 300 pN. A tip force of 50 pN gave heights close to 25 nm, while at forces close to 300 pN the height of the MTs was found to be about 21 nm. A systematic study of the elastic response of MTs in this geometry has been published elsewhere (de Pablo et al. 2003a). Scanning forces around 100 pN provided good resolution without risking destruction.

Single-protein resolution

Figure 4A presents a high-resolution image of an opened MT showing the inner surface. The striated pattern has a 4 nm periodicity, the size of monomeric tubulin. An image of the outside of an intact MT (Fig. 4B) does not show the monomers in the axial direction, whereas protofilaments, i.e. gaps between monomers in the radial direction, are clearly visible. Fourier transforms of the respective images (insets) confirm the monomer spacing in the inner surface by showing faint intensity at about $1/4\ \mathrm{nm}^{-1}$ (Fig. 4A, inset) while no trace of a signal is seen in the Fourier transform of the image of the outer surface of the MT (Fig. 4B, inset) for monomers in the axial direction.

Defects in the microtubule lattice

The lateral resolution in the images was high enough to reveal lattice defects on the MTs. Figure 5A and Fig. 5B

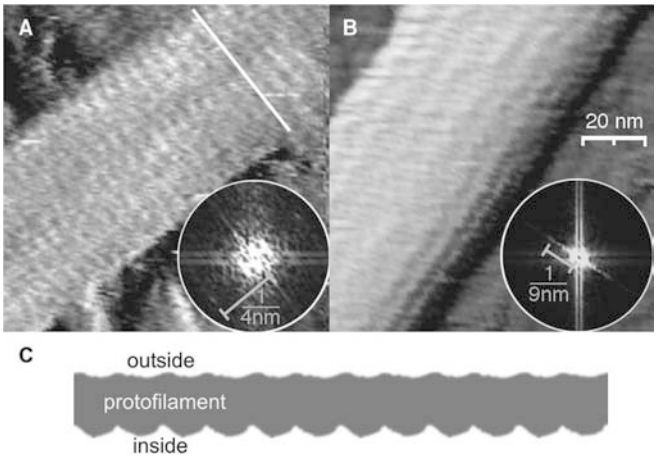

Fig. 4A–C Both scans show a 100×100 nm^2 region scanned with 128×128 points with a maximum tip force of 100 pN. A derivative filter was applied. **A** Opened MT on a DETA surface showing the inner surface of the wall; the protofilaments are hardly visible, but a striated pattern is visible oriented roughly at a right angle to the MT axis. The *inserted line* is exactly perpendicular to the MT axis, showing the angle of the stripes. A fast Fourier transformed image (FFT) (*inset*) shows weak peaks corresponding to a periodicity of 4 nm, the size of a tubulin monomer. **B** Intact MT on an APTS surface showing the outer surface imaged under similar conditions. The protofilaments are visible. Both in the topography as well as in the FFT there is no indication of the axial monomer periodicity. The protofilaments give a visible, but not very clear, signature in the FFT, because only five are visible and their apparent spacing is not constant. **C** Sketch of the axial cross-section of a protofilament based on cryo-EM results by Nogales et al. (1999). The periodicity of the monomers is much more pronounced on the inside. This is consistent with the finding that only an opened MT shows monomer periodicity in the axial direction (see **A**)

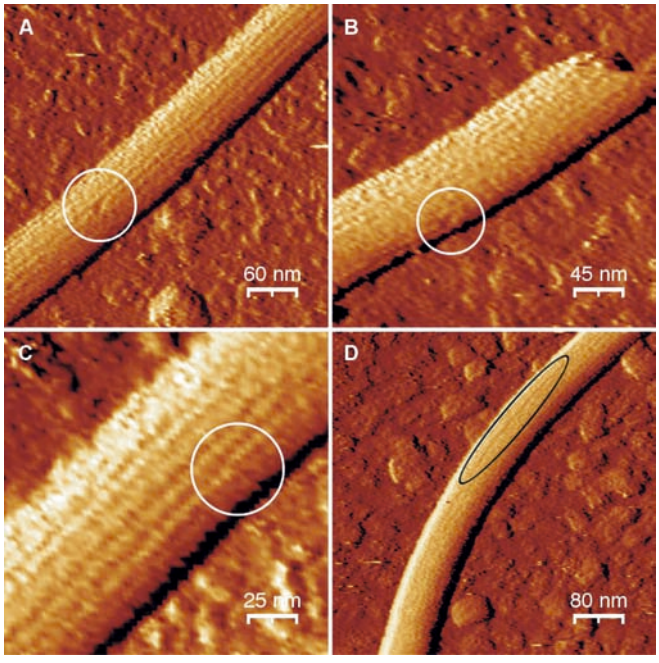

Fig. 5A–D These images were taken with 256 scan points per 500 nm, have a derivative filter applied and were obtained on APTS surfaces. **A** Point defect: one protofilament was disrupted over an apparent length of 12 nm, leaving a hole in the MT wall. The length of the defect (in combination with the dilation) suggests the absence of two tubulin dimers. The MT was scanned three times without observing any change, making it unlikely that scanning had induced or enhanced the defect. **B** Similar point defect as in **A**, but now more to the side of another MT. **C** One (or possibly more) protofilament(s) interrupted by a fracture, after which they continue with a lateral shift. **D** An MT with an unusually small radius of curvature of 650 nm, normally only seen when it is bent by an external force. An increased spacing between protofilaments at the outer side of the curve can be seen, which suggests disrupted lateral bonds

show two point defects, small holes in the MT wall. Figure 5C shows what appears to be a lateral offset in one or more protofilaments or a crack in the wall. Yet another type of defect, a split between two protofilaments, is shown in Fig. 5D. The split is likely related to the relatively strong bend in this MT (radius of curvature 650 nm).

Discussion

The resolution obtained with SFM depends primarily on the size of the tip, while the distance between scan points, combined with the stability of the piezo, as well as Brownian motions of both tip and sample, also play a role. Axial gaps between tubulin monomers could only be detected on the MT inner wall. This is not unexpected, since 3D MT reconstruction from EM data (Nogales et al. 1999) shows virtually no gaps between monomers in the axial direction on the outer protofilament surface, while at the inner surface the tubulin monomers are clearly separated by a cleft (Fig. 4C).

In the so-called B-lattice, in which form microtubules normally polymerize, lateral monomer contacts are primarily between α–α and β–β (Mandelkow et al. 1986). Because neighboring protofilaments are staggered with a pitch of 0.92 nm, the 13-protofilament MT helix has a rise of three tubulin monomers per turn. This implies an axial "seam" with α–β contacts. Evidence has been reported that growing MTs first form as flat ribbons at the growing tip and then progressively curl up to form the closed tubules (Kirschner et al. 1975; Simon and Salmon 1990), leaving a seam with α–β contacts (Kikkawa et al. 1994). This predicted seam was not visible in our SFM images, likely for the reason that we did not resolve differences between α- and β-tubulin. This is consistent with the high homology in tertiary structure found between the two types of monomers, with differences of only ~0.1 nm (Nogales et al. 1998). The split observed in Fig. 5D might be marking the seam, but in this case the radius of curvature of the MT was so short (650 nm) that the opening of the tube might have occurred between any pair of protofilaments in the highly strained MT.

The origin of the point defects we detected might lie in the assembly process, conceivably caused by the inclusion of damaged building blocks (tubulin dimers) or by the fast growth skipping isolated sites. Defects could also be induced by external forces that exceed the

elastic limits of the tube, for example by the SFM tip, or by pipetting of the MT sample before depositing it in on the substrate surface. The defect observed in Fig. 5A was stable over repeated scans at low force, so that it is unlikely that it was caused by the imaging process itself. The number of defects observed so far was too small for a statistical analysis.

The existence of point defects has been indirectly inferred previously in experiments with the motor-protein related protein katanin, an MT severing protein complex (McNally and Vale 1993). Katanin binds the MT, and, by hydrolysis of ATP, disrupts the bonds between tubulin dimers, thereby weakening the MT's lattice. Davis et al. (2002) proposed a model, based on observations of katanin-mediated severing of MTs, in which katanin binds preferentially to defects rather than to random locations. They estimated a frequency of one defect per 0.6 μm, where every postulated defect would correspond to two tubulin dimers. The fact that such defects can exist is demonstrated by our observations, although we cannot give an estimate of the frequency of occurrence due to lack of statistics.

Transitions in protofilament number were found to occur with a frequency of about one per 15–17 μm in cryo-EM studies (Chrétien et al. 1992; Arnal and Wade 1995) under experimental conditions similar to ours (addition of paclitaxel after polymerization). This relatively infrequent occurrence might be the reason why we have not observed any clear examples yet. The shifted protofilament in Fig. 5C could be caused by a change in protofilament number. We did, however, not observe a change in width and height of the MT corresponding to an addition of one protofilament (~5 nm). It is conceivable that our imaging procedure created a bias in the sense that only the most stable MTs might have been visible at all, which are likely to be the ones with 13 protofilaments. If others, however, had been destroyed, we would expect to at least see the remainders of the bottom parts of the tubes, which was not often the case.

The role of paclitaxel for the mechanical properties of microtubules is not yet entirely clear. In our experiments it was used to stabilize the MTs against depolymerization at the low protein concentrations necessary for imaging. Because paclitaxel is a small molecule (MW = 0.85 kD) that binds to a specific location in β-tubulin (Snyder et al. 2001) and does not add a considerable mass, it is not expected to have major effects on the rigidity of the MT. It does, however, influence the frequency of defects. In the absence of paclitaxel, Arnal and Wade (1995) found a protofilament transition rate of one per 35 μm, increasing to one per 6–8 μm when paclitaxel was present during polymerization. In vivo, without paclitaxel, the formation of MTs is an easily reversible process. Although assembly and disassembly is believed to occur predominantly from the ends, it is conceivable that the lattice is more dynamic and that the MT can anneal by dynamic rearrangements of monomers or dimers. Such lattice dynamics might be measurable by the technique we have used. It is likely, however, that the relatively strong attachments needed to image the MTs would prevent some dynamic processes from occurring.

We expect that the presented results, which demonstrate molecular resolution on microtubules in close to physiological conditions, will open new doors to a microscopic understanding of the many complex dynamic machineries that microtubules are involved in.

Acknowledgements We thank Ken Downing for sharing his 3D MT model, Per Bullough for help with image analysis, Fred MacKintosh for helpful discussions, Johanna van Nes and René Koops for help with exploratory experiments, and financial support of the Dutch Foundation for Fundamental Research of Matter (FOM) and ALW/FOM project no. 01FB28/2.

References

Alberts B, Johnson A, Lewis J, Raff M, Roberts K, Walter P (2002) Molecular biology of the cell, 4th edn. Garland, New York

Arnal I, Wade RH (1995) How does Taxol stabilize microtubules? Curr Biol 5:900–908

Binnig G, Quate CF, Gerber C (1986) Atomic force microscope. Phys Rev Lett 56:930–933

Cassimeris L, Spittle C (2001) Regulation of microtubule-associated proteins. Int Rev Cytol 210:163–226

Chretien D, Metoz F, Verde F, Karsenti E, Wade RH (1992) Lattice defects in microtubules: protofilament numbers vary within individual microtubules. J Cell Biol 117:1031–1040

Davis LJ, Odde DJ, Block SM, Gross SP (2002) The importance of lattice defects in katanin-mediated microtubule severing in vitro. Biophys J 82:2916–2927

de Pablo PJ, Colchero J, Gomez-Herrero J, Baro AM (1998) Jumping mode scanning force microscopy. Appl Phys Lett 73:3300–3302

de Pablo PJ, Schaap IAT, MacKintosh FC, Schmidt CF (2003a) Deformation and collapse of microtubules on the nanometer scale. Phys Rev Lett 91:098101

de Pablo PJ, Schaap IAT, Schmidt CF (2003b) Observation of microtubules with scanning force microscopy in liquid. Nanotechnology 14:143–146

Fritz M, Radmacher M, Allersma MW, Cleveland JP, Stewart RJ, Hansma PK, Schmidt CF (1995) Imaging microtubules in buffer solution using tapping mode atomic force microscopy. Proc SPIE 2384:150–157

Gittes F, Schmidt CF (1998) Thermal noise limitations on micromechanical experiments. Eur Biophys J 27:75–81

Hirokawa N (1998) Kinesin and dynein superfamily proteins and the mechanism of organelle transport. Science 279:519–526

Kikkawa M, Ishikawa T, Nakata T, Wakabayashi T, Hirokawa N (1994) Direct visualization of the microtubule lattice seam both in vitro and in vivo. J Cell Biol 127:1965–1971

Kirschner MW, Honig LS, Williams RC (1975) Quantitative electron microscopy of microtubule assembly in vitro. J Mol Biol 99:263–276

Mandelkow EM, Schultheiss R, Rapp R, Muller M, Mandelkow E (1986) On the surface lattice of microtubules: helix starts, protofilament number, seam, and handedness. J Cell Biol 102:1067–1073

McNally FJ, Vale RD (1993) Identification of katanin, an ATPase that severs and disassembles stable microtubules. Cell 75:419–429

Nogales E, Wolf SG, Downing KH (1998) Structure of the alpha beta tubulin dimer by electron crystallography. Nature 391:199–203

Nogales E, Whittaker M, Milligan RA, Downing KH (1999) High-resolution model of the microtubule. Cell 96:79–88

Pierson GB, Burton PR, Himes RH (1978) Alterations in number of protofilaments in microtubules assembled in vitro. J Cell Biol 76:223–228

Simon JR, Salmon ED (1990) The structure of microtubule ends during the elongation and shortening phases of dynamic instability examined by negative-stain electron microscopy. J Cell Sci 96:571–582

Snyder JP, Nettles JH, Cornett B, Downing KH, Nogales E (2001) The binding conformation of Taxol in beta-tubulin: a model based on electron crystallographic density. Proc Natl Acad Sci USA 98:5312–5306

Tilney LG, Bryan J, Bush DJ, Fujiwara K, Mooseker MS, Murphy DB, Snyder DH (1973) Microtubules: evidence for 13 protofilaments. J Cell Biol 59:267–275

Turner DC, Chang C, Fang K, Brandow SL, Murphy DB (1995) Selective adhesion of functional microtubules to patterned silane surfaces. Biophys J 69:2782–2789

Villarrubia JS (1997) Algorithms for scanned probe microscope image simulation, surface reconstruction, and tip estimation. J Res Natl Inst Stand Technol 102:425–454

Vinckier A, Dumortier C, Engelborghs Y, Hellemans L (1996) Dynamical and mechanical study of immobilized microtubules with atomic force microscopy. J Vac Sci Technol B 14:1427–1431

Williams RC Jr, Lee JC (1982) Preparation of tubulin from brain. Methods Enzymol 85:376–385